Archives of Toxicology (2020) 94:219–229
https://doi.org/10.1007/s00204-019-02582-8

ORGAN TOXICITY AND MECHANISMS

The pyrrolizidine alkaloid senecionine induces CYP-dependent destruction of sinusoidal endothelial cells and cholestasis in mice

Stefanie Hessel-Pras[1] · Albert Braeuning[1] · Georgia Guenther[2] · Alshaimaa Adawy[2] · Anne-Margarethe Enge[1] · Johanna Ebmeyer[1] · Colin J. Henderson[3] · Jan G. Hengstler[2] · Alfonso Lampen[1] · Raymond Reif[2]

Received: 1 July 2019 / Accepted: 18 September 2019 / Published online: 12 October 2019

Abstract

Pyrrolizidine alkaloids (PAs) are widely occurring phytotoxins which can induce severe liver damage in humans and other mammalian species by mechanisms that are not fully understood. Therefore, we investigated the development of PA hepatotoxicity in vivo, using an acutely toxic dose of the PA senecionine in mice, in combination with intravital two-photon microscopy, histology, clinical chemistry, and in vitro experiments with primary mouse hepatocytes and liver sinusoidal endothelial cells (LSECs). We observed pericentral LSEC necrosis together with elevated sinusoidal marker proteins in the serum of senecionine-treated mice and increased sinusoidal platelet aggregation in the damaged tissue regions. In vitro experiments showed no cytotoxicity to freshly isolated LSECs up to 500 µM senecionine. However, metabolic activation of senecionine by preincubation with primary mouse hepatocytes increased the cytotoxicity to cultivated LSECs with an EC_{50} of approximately 22 µM. The cytochrome P450 (CYP)-dependency of senecionine bioactivation was confirmed in CYP reductase-deficient mice where no PA-induced hepatotoxicity was observed. Therefore, toxic metabolites of senecionine are generated by hepatic CYPs, and may be partially released from hepatocytes leading to destruction of LSECs in the pericentral region of the liver lobules. Analysis of hepatic bile salt transport by intravital two-photon imaging revealed a delayed uptake of a fluorescent bile salt analogue from the hepatic sinusoids into hepatocytes and delayed elimination. This was accompanied by transcriptional deregulation of hepatic bile salt transporters like *Abcb11* or *Abcc1*. In conclusion, senecionine destroys LSECs although the toxic metabolite is formed in a CYP-dependent manner in the adjacent pericentral hepatocytes.

Keywords Hepatotoxicity · Veno-occlusive disease · 2-Photon microscopy · Xenobiotic metabolism · Liver necrosis

Abbreviations

3-MC	3-Methylcholanthrene
ALT	Alanine transaminase
AST	Aspartate transaminase
AU	Arbitrary unit
AUC	Area under the curve
BC	Bile canaliculi
BW	Body weight
LE	Liver extract
CLF	Cholyl-lysyl-fluorescein
CYP	Cytochrome P450 monooxygenase(s)
GFP	Green fluorescent protein
CV	Central vein
HE	Hematoxylin-eosin staining
KH buffer	Krebs–Henseleit buffer
LSEC	Liver sinusoidal endothelial cells
NPC	Non-parenchymal cells
PI	Propidium iodide
PA(s)	Pyrrolizidine alkaloid(s)

Stefanie Hessel-Pras and Albert Braeuning equally contributed to this work.

Electronic supplementary material The online version of this article (https://doi.org/10.1007/s00204-019-02582-8) contains supplementary material, which is available to authorized users.

✉ Stefanie Hessel-Pras
stefanie.hessel-pras@bfr.bund

[1] Department Food Safety, German Federal Institute for Risk Assessment, Max-Dohrn-Str. 8-10, Berlin, Germany

[2] Leibniz Research Centre for Working Environment and Human Factors, Technical University Dortmund, Ardeystraße 67, Dortmund, Germany

[3] Systems Medicine, Jacqui Wood Cancer Centre, University of Dundee, School of Medicine, James Arrott Drive, Ninewells Hospital, Dundee, UK

PMH	Primary mouse hepatocytes
POR	NADPH-cytochrome P_{450} reductase
$t_{1/2}$	Half-life
t_{max}	Time to maximum
TMRE	Tetramethylrhodamine ethyl ester
VOD	Veno-occlusive disease

Introduction

More than 660 different pyrrolitidine alkaloids (PAs) have been identified, about half of them are known to be hepatotoxic (Fu et al. 2004; Stegelmeier et al. 1999). Plants typically contain mixtures of PAs, of which the 1,2-unsaturated form, like senecionine, exhibits the strongest hepatotoxic properties. Their genotoxicity and carcinogenicity are based on the metabolic activation of 1,2-unsaturated PAs to highly reactive, electrophilic pyrrole derivatives by cytochrome P450 (CYP) monooxygenases (Fu et al. 2004). Human exposure to PAs predominantly occurs through consumption of PA-containing plants, food prepared from PA-contaminated materials, tea, and honey (Bodi et al. 2014; Mulder et al. 2015). Epidemic PA poisoning occurred in central India in 1975 due to the consumption of millet contaminated with seeds of *Crotalaria* species. Around 8000 individuals were affected by *Heliotropium popovii* contamination of bread in 1975/1976 in Afghanistan, with 3000 severe intoxications and a relatively high mortality rate. Another outbreak of hepatic VOD due to the consumption of *Heliotropium popovii*-contaminated bread occurred 2008 in Afghanistan (Kakar et al. 2010). Typical histological consequences of PA intoxication are centrilobular hemorrhagic necrosis and fibrosis, and veno-occlusive disease (VOD). Clinical symptoms accompanying VOD comprise ascites, edemas, hepatomegaly, emaciation and an increase of blood bilirubin levels which may result in jaundice (Mohabbat et al. 1976; Tandon et al. 1978; WHO 1988).

A number of publications (Luckert et al. 2015; Waizenegger et al. 2018; Yang et al. 2016) have analyzed the impact of PAs on hepatocytes, the most abundant hepatic cell type and main target of most hepatotoxins. Analyses of PA-treated human primary hepatocytes identified numerous hepatotoxic pathways like hepatic steatosis, cholestasis, hepatomegaly, inflammation and cancer-associated signaling pathways as affected by PA exposure (Luckert et al. 2015). Many studies also showed PA cytotoxicity and the induction of apoptosis in vivo and in vitro in different cell systems (Copple et al. 2004; Ebmeyer et al. 2019c; Gordon et al. 2000; Steenkamp et al. 2001; Waizenegger et al. 2018). However, VOD as a typical marker of PA poisoning also suggests the induction of effects in other cell types than hepatocytes, especially in endothelial cells (Chen and Huo 2010; DeLeve et al. 2002). Based on a rat VOD model using the PA monocrotaline, it has been suggested that endothelial cells round up, detach, and finally embolize to block the microcirculation (DeLeve et al. 2002). However, the molecular mechanisms responsible for this key event remain unclear. In vitro data suggest that endothelial cells may be more susceptible to reactive PA intermediates and this difference may be related to the lower levels of the important scavenger glutathione (Yang et al. 2016). Accordingly, glutathione infusion was shown to prevent hepatotoxicity of the PA monocrotaline (Wang et al. 2000). Moreover, matrix metalloproteinases appear to be involved in PA toxicity in endothelial cells (Deleve et al. 2003b).

Many details of PA-dependent hepatotoxicity have not been elucidated yet in depth, especially with respect to the mechanisms of VOD development. Therefore, the present study was designed to address three key questions, namely to unravel the mechanisms by which senecionine induces cholestasis, to elucidate whether the in vivo hepatotoxicity of senecionine is CYP-dependent, and to determine how the liver sinusoidal endothelial cells are affected by the compound.

Materials and methods

Animals and materials

All animals and materials used in this study are summarized in Table S1 in supplemental material.

Animal study and sample collection

Intravital imaging and hepatotoxicity studies were performed using male C57BL/6NRj mice. In addition, Tie2 reporter mice were used for the visualization of the sinusoidal cells and platelets in intravital imaging. These mice were derived from mating Tie2Cre mice (Koni et al. 2001) with mT/mG mice (Muzumdar et al. 2007) expressing eGFP in the target cells. To test for cytochrome P450 (Cyp)-dependent bioactivation of senecionine, endogenous reductase locus (ERL) mice were used. These mice carry a floxed NADPH-cytochrome P450 reductase (POR) and Cre recombinase under the control of the *Cyp1a1* promoter. POR-knockout was induced by intraperitoneal (i.p.) injection of 4 mg per kg BW of the Cyp1a1 inducer 3-methylcholanthrene (3-MC) 10 days prior to senecionine administration (Henderson et al. 2015). For all experiments male mice were used at the age of 8–10 weeks. Animals were housed with 12 h light–dark cycle and provided ad libitum access to water and standard mouse diet (Ssniff, Soest, Germany). All animal experiments were approved by the local authorities (LANUV, Recklinghausen, Germany). All details for treatment of animals, quantitative analysis of histological

staining, the pharmacokinetic analyses of cholyl-lysyl-fluorescein (CLF) elimination, the immunohistochemistry and Western blotting, as well as the isolation of RNA and quantitative real-time PCR are described in detail in the supplementary material.

Intravital imaging

Intravital imaging was performed according to a previously published procedure (Reif et al. 2017). In brief, Hoechst 33,258 and propidium iodide (PI) were injected into anesthetized mice via the tail vein. C57BL/6NRj mice additionally received tetramethylrhodamine ethyl ester (TMRE). A small midline incision was introduced in the upper abdomen and the falciform ligament was cut to expose the left liver lobe. The mouse was laterally placed onto a 0.17-mm-thick cover slip (Logitech Limited, Glasgow, UK) in a custom-made platform. For the online injection of CLF a lateral tail vein was catheterized (SAI Infusion Technologies, Lake Villa, USA). Images were acquired using a custom-modified inverted LSM MP7 (Zeiss, Göttingen, Germany) with LD C-Apochromat 40 × 1.1 water immersion objective (Zeiss, Göttingen, Germany). During imaging the animal was kept under 0.5–1% isoflurane with an evaporator (Foehr Medical Instruments, Seeheim-Jungenheim, Germany) and maintained at 37 °C in an incubation chamber (Solent Scientific, Portsmouth, UK). For two-photon excitation, a Chameleon Ultra II laser (Coherent, Gilching, Germany) tuned to 780 nm was used. The blue fluorescence was collected in a NDD detector using the shortpass filter 485, the green and the red fluorescence were collected in a GaAsP detector with the bandpass filters 500–550 and 565–610, respectively. Imaging was performed with a dwell time between 1 and 3 µs and a frame rate of 5–15 s per scan.

Senecionine toxicity in vitro

Primary mouse hepatocytes (PMH) were isolated as described previously (Reif et al. 2015). In brief, the liver of a C57BL/6NRj mouse was initially perfused with EGTA buffer (Krebs–Henseleit (KH) supplemented with 0.51 mM EGTA, pH 8.2) and subsequently changed to collagenase buffer (KH buffer with 5.1 mM $CaCl_2$, 45.5 U collagenase per ml (#C2674, Sigma Aldrich, Taufkirchen, Germany), pH 8.2). After perfusion, the liver was dissected and gently dissociated in suspension buffer (KH buffer supplemented with 1.05 mM $CaCl_2$, 0.4 mM $MgSO_4$, 2% BSA, pH 7.4). The resulting cell suspension was first filtered through a strainer (pore size 100 µm) and centrifuged at 50 × *g* for 5 min at 4 °C. The pellet contained the PMH fraction. The supernatant was centrifuged again at 400 × *g* for 10 min at 4 °C to pellet the non-parenchymal cell (NPC) fraction. Both pellets were resuspended in suspension buffer. 150,000 PMHs or 1.5 million NPCs were seeded per well in a 4-well µ-slide chamber pre-coated with a collagen IV (Ibidi, Martinsried, Germany) in cultivation medium (Williams E medium, PAN Biotech) supplemented with 2 mM glutamine, 100 U/ml penicillin, 0.1 mg/ml streptomycin, 10 µg/ml gentamycin (all PAN Biotech, Aidenbach, Germany), 100 nM dexamethasone, 20 ng/ml bovine insulin (both Sigma Aldrich, Taufkirchen, Germany), 50 ng/ml murine EGF (R&D Systems, Minneapolis, USA) and 10% sera plus (PAN Biotech, Aidenbach, Germany). After 3 h of attachment, medium was changed to serum-free cultivation medium containing senecionine in concentrations between 0 and 500 µM. In case of a medium transfer, the supernatants of the PMH cultures were transferred to the corresponding NPC cultures after 6 h. Cells were treated for 2 days before the CellTiter-Blue viability assay (Promega, Mannheim, Germany) was performed according to the manufacturer's instructions. The PMH and the NPC cultures were incubated with the fluorogenic substrate for 1 h or 5 h, respectively. The resulting fluorescence intensity was measured with an Infinite M200 Pro plate reader (Tecan, Tecan Group, Maennedorf, Switzerland) at 540 nm for excitation and 594 nm for emission.

Statistical analysis

Significant differences between mean values in a concentration- or time-series were calculated by one-way analysis of variance (ANOVA) followed by Dunnett's post hoc test versus the corresponding control or the time point 0 h. Scenarios including two variables were analyzed by two-way ANOVA (gene expression analysis) or two-way ANOVA followed by Holm–Sidak post hoc test (kinetic parameters). Comparison of mean values between two groups was analyzed by Student's t test. Normal distribution was assumed for all data. Statistically significant differences are indicated by asterisks: $*p < 0.05$, $**p < 0.01$, $***p < 0.001$.

Results

LSEC necrosis, hemorrhage, and platelet aggregation are characteristics of senecionine intoxication

In order to gain a better understanding of the mechanisms underlying the hepatotoxicity of PAs, we used senecionine as a representative test compound. Senecionine is one of the most frequently occurring PA in tea samples (Bodi et al. 2014) also exhibiting high potency to induce strong toxicity (Merz and Schrenk 2016). Initially, time- and dose-dependent hepatotoxicity of senecionine was analyzed in C57BL/6NRj mice. Both liver diagnostic markers ALT and AST emerged in blood 18 h after oral administration of

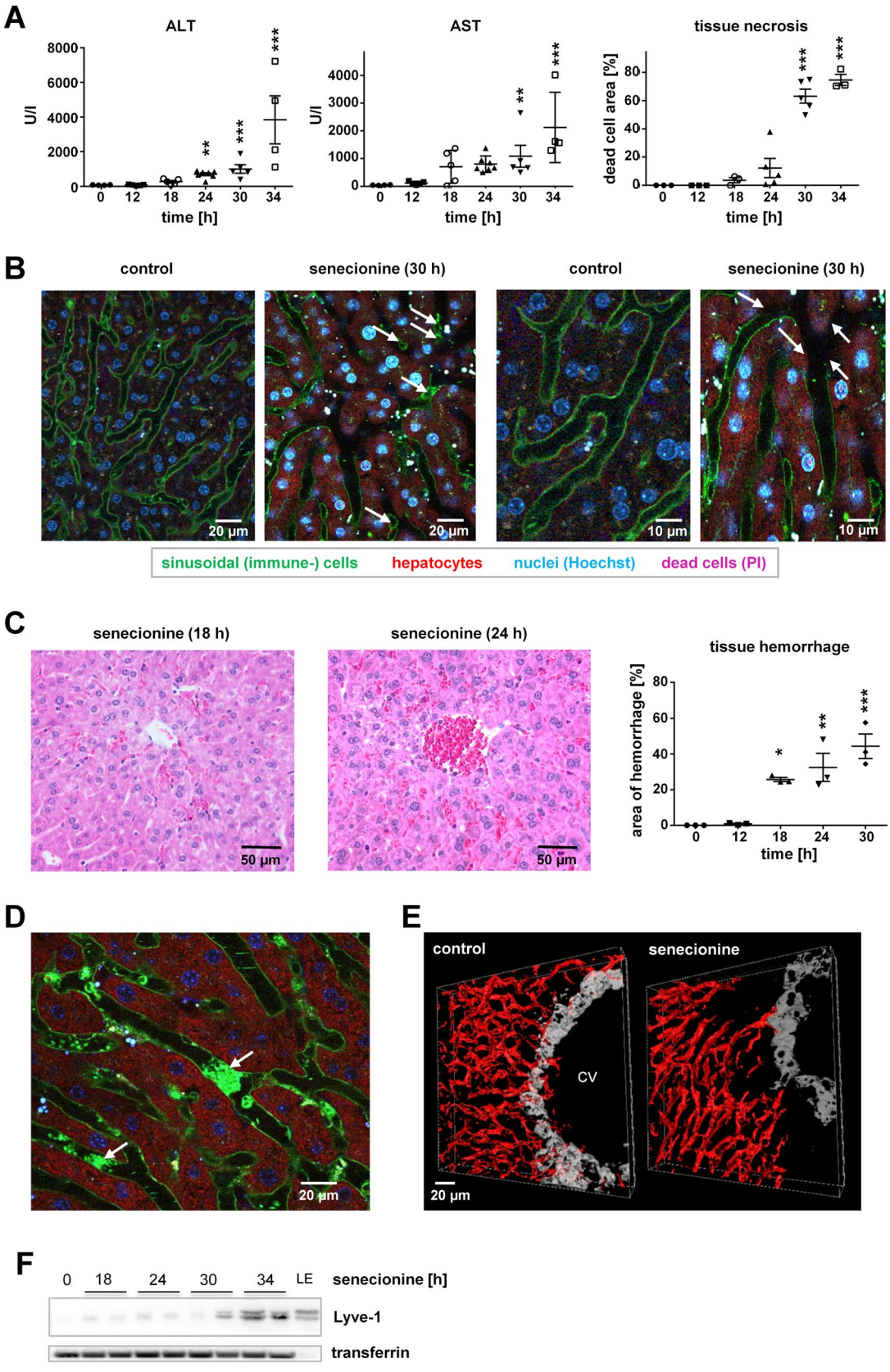
A
ALT
AST
tissue necrosis
U/l
dead cell area [%]
time [h]
B
control
senecionine (30 h)
control
senecionine (30 h)
20 µm
10 µm
sinusoidal (immune-) cells
hepatocytes
nuclei (Hoechst)
dead cells (PI)
C
senecionine (18 h)
senecionine (24 h)
tissue hemorrhage
area of hemorrhage [%]
50 µm
D
20 µm
E
control
senecionine
CV
20 µm
F
0
18
24
30
34
LE
senecionine [h]
Lyve-1
transferrin

◂**Fig. 1** Toxic effects induced by senecionine in mouse liver. **a** Administration of 60 mg senecionine per kg BW resulted in increasing AST and ALT serum levels associated with marked tissue necrosis. **b** Specific loss of pericentral LSECs (arrowheads) in senecionine-treated Tie2 reporter mice compared to control animals (left), accompanied by infiltration of immune cells (arrows). **c** Histology of senecionine-treated mice showed pericentral hemorrhage which extended over time. **d** Intravital imaging of Tie2 reporter mice illustrated transient platelet aggregation (arrows). See also Supporting Video 1 for senecionine-treated mouse and Supporting Video 2 for control Tie2 reporter mouse. **e** Sinusoidal reconstruction of control and senecionine-treated mice (time point 24 h) demonstrates LSEC loss in the pericentral region. **f** Lyve-1 was identified as a serum marker for LSEC destruction in senecionine-treated mice (LE, liver tissue extract from freshly isolated untreated mouse). Statistical relevance was determined using ANOVA followed by Dunnett's post hoc test against $t=0$ h with p values as follows: *<0.05, **<0.01, ***<0.001

60 mg senecionine per kg BW and increased notably over the investigated time (Fig. 1a). After 30 h, clinical symptoms of the senecionine-treated mice were evident. Pericentral necrosis was first observed 18 h after senecionine administration in HE-stained liver sections and increased up to a dead cell area of approximately 75% after 34 h, extending in some mice into the midzonal lobular region (Fig. 1a, right panel). In a dose-dependent experiment, markers of hepatotoxicity were unchanged in animals with 15 mg/kg BW after 30 h compared to control animals (Supporting Fig. S1A–C). Higher doses up to 60 mg/kg led to constantly increasing ALT and AST levels. Similarly, in histopathology approximately 20% of the pericentral region was necrotic with 45 mg/kg BW after 30 h, reaching 65% with 60 mg/kg BW. Hence, we chose 60 mg senecionine per kg BW to study senecionine-induced hepatotoxic effects in more detail. The observations described above were corroborated by findings at the gene expression level, demonstrating a senecionine-dependent loss of expression of genes expressed in the pericentral lobular zone, such as *Cyp1a2*, *Cyp2e1*, *Axin2*, *Lgr5*, and *Cyp7a1* (Fig. 2). Intravital two-photon microscopy (Denk et al. 1990; Helmchen and Denk 2005) was used for the first time to study PA hepatotoxicity in mouse liver. The Tie2 reporter mouse which expresses red fluorescent membrane-bound tdTomato in hepatocytes as well as green fluorescent membrane-bound GFP in sinusoidal cells, platelets, and immune cells was chosen in order to differentiate between the liver cell types (Constien et al. 2001). Fluorescence microscopy of livers from senecionine-treated Tie2 reporter mice revealed a remarkable pericentral loss of liver sinusoidal endothelial cells (LSECs) 30 h after intoxication (Fig. 1b). Immune cell infiltration into the tissue accompanied LSEC depletion (Fig. 1b, right). Accordingly, a time- and dose-dependent induction of the inflammation-related mRNAs for *Lcn2*, *Mt2* and *Saa3* were observed (Fig. 2). Hepatic hemorrhage was detected in the pericentral region from 18 h on, while the area of hemorrhage extended gradually over the investigated time of 24 h (Fig. 1c). Moreover, transient aggregation of platelets occurred more frequently in senecionine-exposed mice than in controls during in intravital imaging of Tie2 reporter mice (Fig. 1d, Supporting Video 1 and 2). Three-dimensional reconstruction of liver sinusoids was used to illustrate the pericentral LSEC loss (Fig. 1e). The intravital recordings clearly show the zone-specific pericentral degeneration of LSECs as a fundamental early effect of senecionine intoxication. Tissue hemorrhage and platelet aggregation occurred simultaneously as a consequence of the loss of the liver endothelium.

Metabolic activation of senecionine by Cyps is a precondition of LSEC destruction

Intoxications caused by xenobiotics often result from their metabolic activation by cytochrome P450 (Cyp) enzymes in hepatocytes (Park et al. 2005). Therefore, we addressed the question next whether the toxic effect of senecionine on LSECs originates from the parental compound or from active metabolites. To study the impact of Cyp-mediated metabolism on senecionine toxicity, mice deficient in hepatic NADPH-cytochrome P450 oxidoreductase (POR) which in the active state mediates the electron transfer from $NADPH/H^+$ to Cyp was utilized. Deficiency in POR results in a strongly reduced activity of Cyp. HE-stained liver sections from (3-MC-treated) POR-knockout mice that were exposed to 60 mg senecionine per kg BW for 36 h were identical to the control sections of the untreated mice (Fig. 3a) Accordingly, the levels of the diagnostic markers ALT and AST in the blood of POR-knockout mice were not elevated compared to solvent-treated animals (Fig. 3b). In contrast to C57BL/6NRj mice, senecionine did not cause necrotic areas or signs of tissue hemorrhage in mice with POR deletion. These results indicate that senecionine requires metabolic activation to induce its toxic effect.

Subsequent in vitro experiments with primary mouse hepatocytes (PMH) and primary LSECs were conducted to study whether the LSEC-harming compound originates from Cyp-mediated metabolism in the hepatocytes. Isolated LSECs (NPCs) displayed no signs of toxicity when exposed to non-metabolized senecionine in concentrations up to 500 µM (Fig. 3c, red). In contrast, PMH showed a concentration-dependent decrease in viability throughout the tested senecionine concentrations with an EC_{50} value of 26 µM (Fig. 3c, blue). NPCs exposed to PMH-conditioned senecionine-containing medium showed a similar toxic response as the PMH cultures, with an EC_{50} of 22 µM (Fig. 3c, green). Moreover, senecionine had no effect on the viability of PMH derived from POR-knockout mice up to a concentration of 200 µM; only upon exposure to 500 µM the viability of POR-knockout PMH decreased to approximately 60% (Fig. 3c, black). These findings demonstrate that

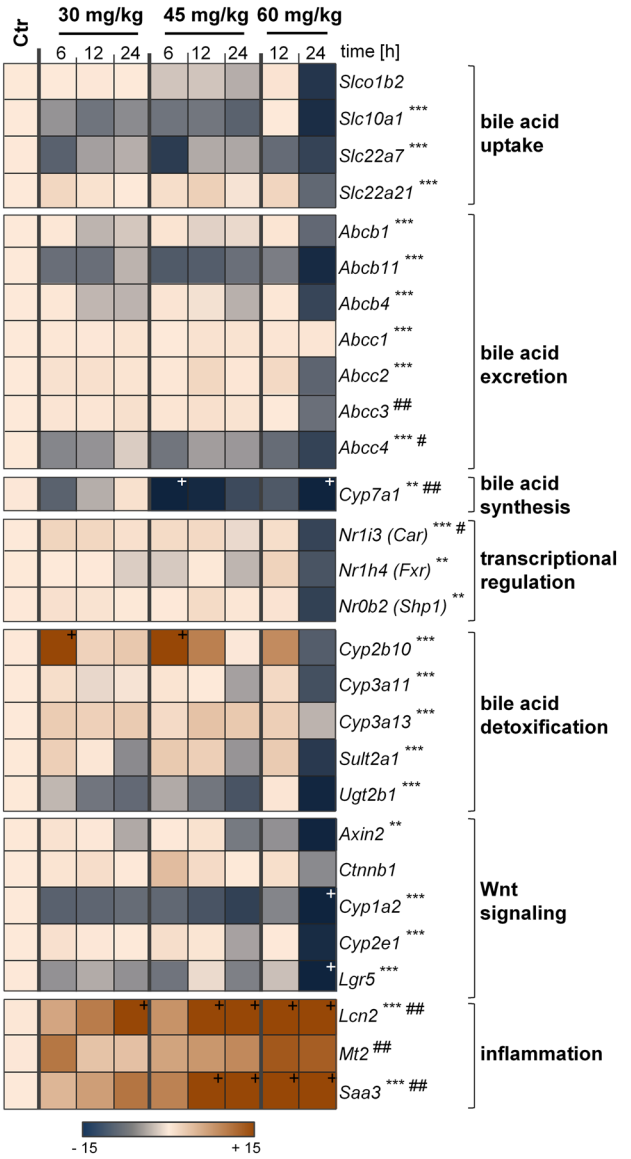

Fig. 2 Influence of senecionine on hepatic gene expression. Expression of hepatic genes involved in bile acid homeostasis, WNT signaling and inflammatory response was affected. Senecionine mainly caused a concentration-dependent decrease in expression of bile acid homeostasis-associated genes with overall lowest mRNA levels at the highest tested dose (60 mg/kg BW) after 24 h with a simultaneous increase of the inflammatory response. Both effects may be associated with the dose-dependent induction of pericentral necrosis. Relative mRNA gene expression values are expressed as means with $n=5$ for 6 h, 12 h and 24 h treatment with 30 mg/kg BW and 6 h treatment with 45 mg/kg BW or $n=4$ for remaining treatments. Statistical relevance was determined two-way ANOVA with p values as follows: *< 0.05, **< 0.01, ***< 0.001 (*time dependence; #dose dependence). Relative gene expression below − 15 or above 15 is indicated by +

senecionine is metabolically activated by Cyps in hepatocytes and the resulting metabolite(s) of senecionine (in conditioned medium) are sufficiently stable to harm neighboring LSECs.

Mice exposed to senecionine develop cholestasis

Bile acid concentrations in blood were elevated 18 h after senecionine administration and further increased at later time points (Fig. 4a). In contrast, ERL mice with POR-knockout showed similar bile acid concentrations compared to control animals. Tracing the transport of the bile salt analogue CLF was used to determine the kinetic differences of bile acid uptake and excretion between control and senecionine-treated mice in vivo. Before recording the nuclear marker Hoechst 33,258, the nuclear marker PI, and the mitochondrial potential marker TMRE were injected (Fig. 4b).

In control mice, CLF was detected in the sinusoids approximately 0.2 min after injection. Next, CLF was enriched at the margin between sinusoidal endothelial cells and hepatocytes (Fig. 3b, 0.5 min), which probably represents the space of Disse, followed by enrichment in hepatocytes throughout the entire liver lobule approximately 1.5 min post-injection with higher intensity of the signal in the pericentral region (Fig. 4b upper, Supporting Video 3). Intracellular CLF was then exported into the bile canaliculi where it reached maximal intensity between 1 and 10 min after injection. Approximately 12.5 min after injection, fluorescence of CLF was exclusively present in bile canaliculi, and to a large part eliminated from the liver. The CLF signal was almost completely cleared from the liver of the control mice approximately 60 min after tail vein injection.

The kinetics of CLF uptake and transport into the hepatocytes and bile canaliculi were altered upon senecionine treatment (Fig. 4b bottom, Supporting Video 4). Only few PI positive cells were observed in the pericentral region (arrow). The half-life of CLF in the sinusoids was prolonged and a lack of the transient enrichment in the pericentral sinusoidal cells compared to control mice was observed. Transport of CLF from the hepatocytes into the bile canaliculi was strongly delayed in the pericentral hepatocytes. Bile canaliculi appeared widened especially in the pericentral region (arrowheads). CLF enriching hepatocytes with positive nuclear PI staining failed to excrete CLF into bile canaliculi.

In summary, senecionine caused a delay of CLF uptake from the sinusoids and excretion into the canaliculi resulting in increased bile acid concentrations in all compartments of the liver lobule, as quantified by CLF fluorescence (Fig. 4c) and subsequently calculated kinetic parameters T_{max}, AUC, and $T_{1/2}$ (Fig. 4d).

At the gene expression level, significant alterations in mRNA expression related to bile acid synthesis, metabolism and transport were detected after exposure to senecionine (Fig. 2): expression of several solute carrier-class transporters (*Slco1b2, Slc10a1, Slc22a7, Slc22a21*) involved in bile acid uptake into hepatocytes was reduced, and similar observations were made for ABC transporters involved in bile acid excretion (*Abcb1, Abcb11, Abcb4, Abcc2, Abcc4*). However,

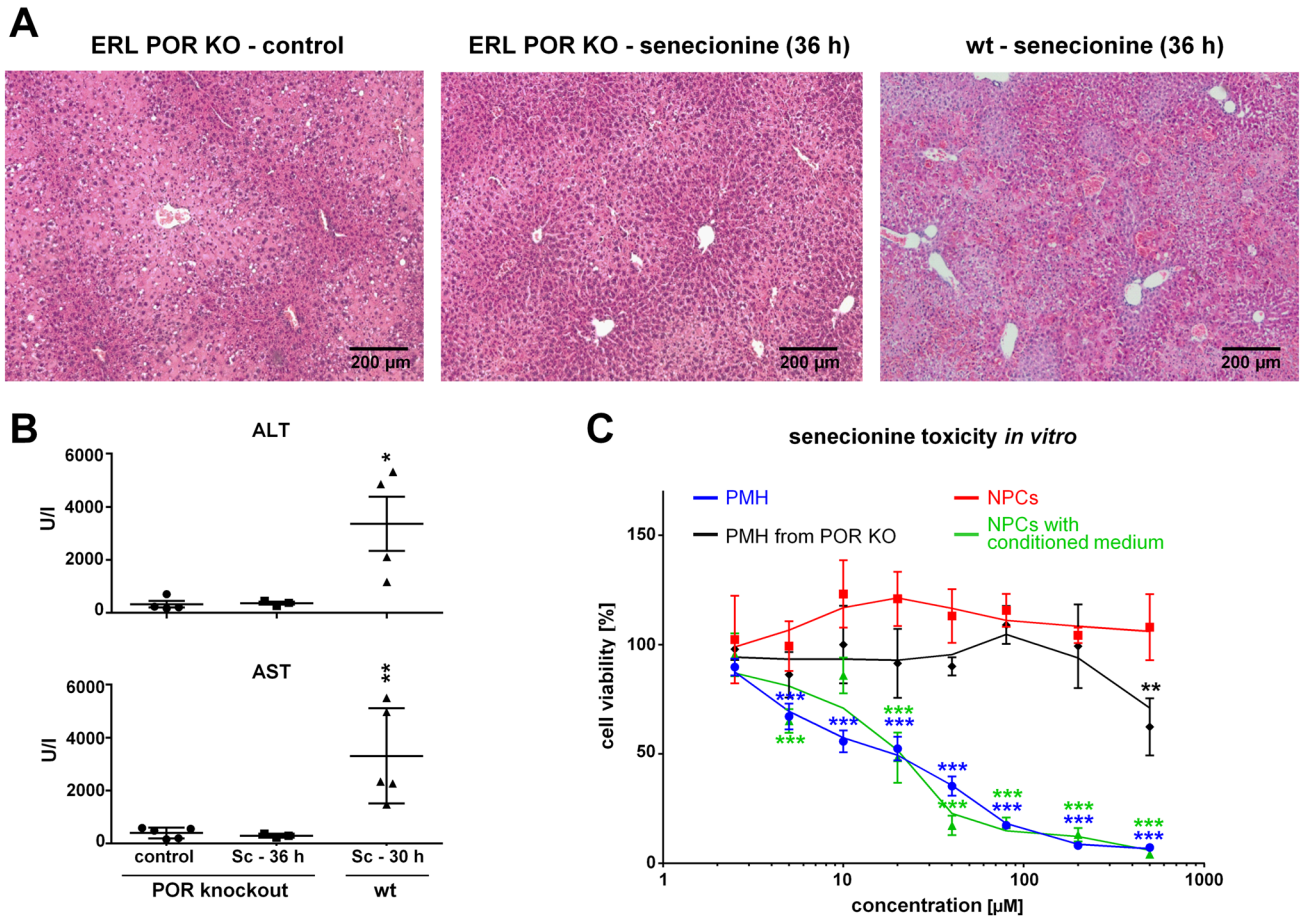

Fig. 3 Senecionine toxicity is cytochrome P450 reductase-dependent and affects hepatocytes and LSECs. **a** ERL mice induced with MC for POR-knockout (POR KO) showed no liver necrosis after 60 mg senecionine per kg BW administration in contrast to C57BL/6NRj mice. **b** ALT, AST, and bile acid serum levels in POR-knockout mice were similar to control levels. **c** PMHs from wt mice showed a concentration-dependent decrease in viability with increasing senecionine concentrations up to 500 µM (blue), while isolated LSECs (wt) were not affected by senecionine in the tested concentrations (red). LSECs cultivated in senecionine conditioned medium derived from PMHs lost viability similarly as wt hepatocytes (green). PMHs from POR KO mice were resistant to senecionine up to a concentration of 200 µM (black). Statistical significance was determined using ANOVA followed by Dunnett's post hoc test against $t=0$ h with p values *<0.05, **<0.01, ***<0.001 (**c**) or student's t test with p values *<0.05, **<0.01 (treatment vs control in respective mouse strain)

Abcc1 involved in bilirubin and conjugated bile salt excretion was identified to be time-dependent significantly up-regulated (supplemental material Fig. S2). Expression of genes associated with the of bile homeostasis was significantly downregulated after treatment with 60 mg senecionine per kg BW at 24 h. Likewise, genes associated with pericentral Wnt signaling were downregulated.

Discussion

The present study provides for the first time, real-time insight into hepatotoxic injury caused by PAs. Early pericentral destruction of LSECs in VOD development and dependence of this process on metabolic activation of the PA senecionine by hepatic Cyp enzymes was demonstrated in vivo. Naturally occurring 1,2-unsaturated PAs can induce severe liver damage in humans and livestock. Case reports, e.g., from a 6-month-old girl who was diagnosed with hepatic VOD progressing to sinusoidal liver fibrosis and cirrhosis, show that an intake of 0.8–1.7 mg PAs per kg BW per day for 2 weeks was sufficient to induce VOD (Stillman et al. 1977; WHO 1988). A 2-month-old boy ingested 3 mg PAs per kg body weight per day and died after 6 days with pronounced centrilobular hemorrhagic necrosis of the liver (Fox et al. 1978; WHO 1988).

Single senecionine doses used in the present mouse study caused acute hepatotoxicity; the highest dose (60 mg/kg BW) is 2–6 times higher compared to the doses reported in the case studies of the above-mentioned intoxicated infants

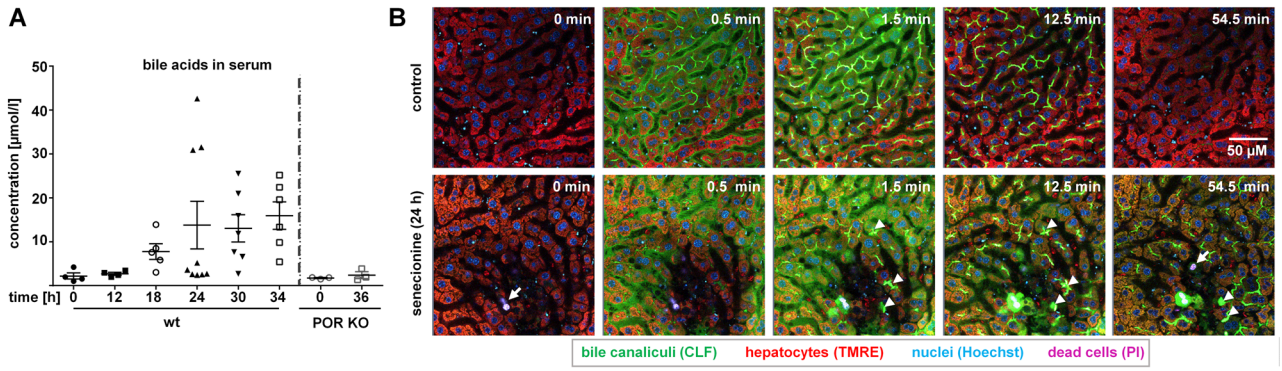

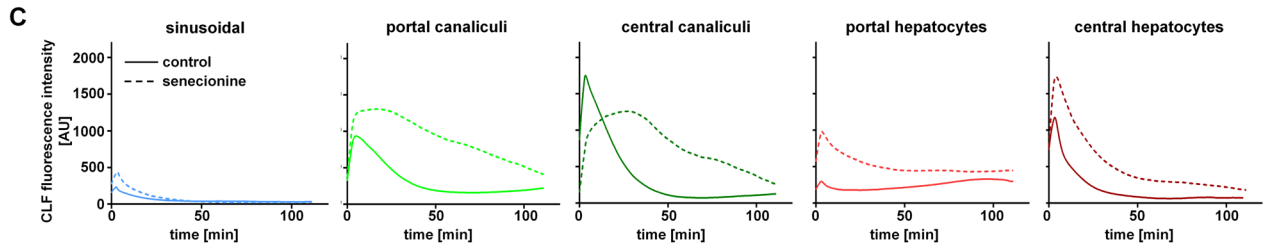

D

	control					senecionine				
	sinusoidal	portal canaliculi	central canaliculi	portal hepatocyte	central hepatocyte	sinusoidal	portal canaliculi	central canaliculi	portal hepatocyte	central hepatocyte
T_{max} [min]	3.0 ± 0.1	8.8 ± 1.0	5.1 ± 0.4	4.6 ± 0.3	5.3 ± 0.4	6.8 ± 2.9	10.0 ± 1.1	12.9** ± 2.8	5.3 ± 0.5	8.9 ± 2.7
AUC [AU x min]	7503 ± 1788	43333 ± 4091	50376 ± 9812	21631 ± 2790	23007 ± 7298	9065 ± 4361	78806* ± 18048	77211 ± 15116	30347 ± 8928	44342 ± 12147
Elimination rate $T_{1/2}$ [min^{-1}]	2.2 ± 0.5	14.6 ± 3.5	9.1 ± 0.8	2.6 ±0.1	2.6 ± 0.6	2.5 ± 0.6	31.4* ± 8.4	32.9** ± 8.9	5.2 ± 1.5	11.5 ± 5.6

Fig. 4 Senecionine intoxication causes cholestasis. **a** Elevated bile acid concentrations were detected in the blood of C57BL/6NRj mice 18 h after administration of 60 mg senecionine per kg BW. **b** Bile acid transport is delayed in senecionine-treated mice. The stills from intravital imaging videos show hepatic clearance of the green fluorescent bile salt analogue CLF of a control mouse (upper, see also Supporting Video 3) and a senecionine-treated mouse after 24 h (bottom, see also Supporting Video 4). The arrow depicts dead cells, with positive nuclear PI staining; arrowheads indicate widened BC. **c** Time-resolved quantification of CLF fluorescence progressing from the sinusoids, into hepatocytes and BC. Quantification differentiates between the pericentral and periportal regions of liver lobules. CLF clearance of control (solid line) and senecionine-treated animals (dashed line) is shown for one representative mouse, while data of all analyzed mice are given in the table (**d**). **d** Table of the determined kinetic parameters time of maximum T_{max}, AUC, and the elimination rate $T_{1/2}$ of CLF fluorescence in the different compartments of the liver, comparing control and senecionine-treated animals. Data are mean values and SD of 5 mice. Statistical significance was determined using two-way ANOVA followed by Holm–Sidak post hoc test against control mice with p values *<0.05, **<0.01

who were exposed in sum over the whole short period of 1 or 2 weeks to 11–25 mg PAs per kg BW. Reported clinical outcomes are comparable between intoxicated mice and human infants comprising the development of severe liver damage including centrilobular necrosis, and the disturbance of bile acid homeostasis which is reflected by jaundice in humans (Fox et al. 1978; Stillman et al. 1977; WHO 1988). In the case report by Datta et al. (1978) two patients developed jaundice, abdominal pain, ascites, gastrointestinal bleeding and hepatic encephalopathy after an estimated daily intake of 3.3 mg of the PA heliotrine per kg BW for 20 or 50 days. Death occurred in the second week or within 12 weeks, respectively (Datta et al. 1978). However, such severe intoxications do not occur frequently. Based on recent data collected in the EU, an estimate upper bound exposure of 820.5 ng PAs per kg BW per day (95th percentile exposure, mean value 310.8 ng/kg BW per day) was calculated for toddlers (EFSA 2016). The chronic exposure to PAs in middle Europe is estimated to range between 34.5 to 48.4 ng per kg BW per day in the young population and between 31.1 to 41.8 ng per kg BW per day in the adult population, with PA-contaminated tea being the main source of exposure (EFSA 2016).

The toxicity of PAs depends on their metabolism in the liver where they can either be metabolically activated or detoxified. Hydrolysis into water-soluble free necine acids and bases and *N*-oxidation of the parent compounds represent the detoxification routes. CYP-dependent dehydrogenation of the pyrrolizidine ring can lead to the conversion of non-cleaved esters into toxic pyrrole derivatives

(dehydropyrrolizidine esters). Pyrrole derivatives are highly reactive alkylating agents capable of binding to nucleic acids and proteins. They can also react with nucleophilic biomolecules after hydrolysis to dehydronecine. As a result of adduct formation, hepatotoxic, carcinogenic and mutagenic effects may occur (Ebmeyer et al. 2019a, b, c; Ruan et al. 2014). Our results showed for the first time that the induction of toxic effects in hepatocytes and LSECs clearly depends on the direct Cyp-mediated activation of senecionine in vivo, as already suggested for PAs like senecionine or lasiocarpine in vitro (Ebmeyer et al. 2019a, b; Ruan et al. 2014). The specific metabolism-dependent destruction of the LSECs was observed in vivo using POR-knockout mice and the in vitro approach demonstrating cytotoxicity on LSEC only after metabolic activation of senecionine using PMH supernatant. The strong toxicity of the metabolized senecionine observed in this study may be associated with a significant depletion of glutathione as reported to occur during the development of the VOD. The continuous administration of glutathione prevents the development of PA-induced VOD in a rat model, and it is therefore assumed that glutathione depletion plays an important role in the development of VOD (DeLeve et al. 2003a; Helmy 2006).

The development of jaundice has often been reported in the context of PA intoxication (Fox et al. 1978; Gao et al. 2012; Stillman et al. 1977; WHO 1988). The present study showed that bile acid concentrations increased after senecionine intoxication in mice. This effect was shown to be Cyp-dependent (Fig. 4a). A comparable increase of bile acids in serum of rats was also observed after oral administration of senecionine and a PA cocktail isolated from *Senecio vulgaris* (Xiong et al. 2014). Also, other case studies of intoxicated livestock showed an increase of bile acids in serum and enhanced bilirubin after ingestion of PA-containing plants (Baker et al. 1991; Mendel et al. 1988; Stegelmeier et al. 1996). Increased serum bile acids may be associated with excessive secretion of bile acids from the liver due to bile acid overload in hepatocytes as observed in mouse hepatocytes using the fluorescent-labeled bile salt cholyl-lysyl-fluorescein (CLF) (Fig. 4). As a consequence, excretion from hepatocytes may be induced and de novo synthesis of bile acids reduced as adaptive response. We identified the basolateral efflux pump *Abcc1* as up-regulated on mRNA level. In rats, an up-regulation of Abcc1 was reported to occur in hepatocytes after bile duct ligation, which may represent an adaptive mechanism of the impaired hepato-biliary excretion of organic anions (Pei et al. 2002). However, in contrast to the study of Xiong et al. (2014) dealing with the effects of senecionine in rats on bile homeostasis (Xiong et al. 2014), no up-regulation of the basolaterally expressed bile acid efflux pump Abcc3 was observed in our study. In the present study all bile acid homeostasis-associated genes were downregulated. This was accompanied by upregulation of inflammation associated genes, such as *Lcn2*, *Mt2* and *Saa3*.

Our study showed severe liver damage in mice including the induction of pericentral necrosis and the disturbance of bile acid homeostasis accompanied with induction of inflammatory processes. Average human exposure of consumers in Western countries, however, is expected to be several orders of magnitude lower than the dose (60 mg senecionine per kg BW) used in the present animal study. Total daily human PA intake with normal nutrition was estimated to be in median 0.019 µg/kg BW for children and 0.026 µg/kg BW for adults. A high uptake was described for the intake of a PA-containing dietary supplements, where a human exposure of about 9 µg/kg BW per day was calculated (Dusemund et al. 2018). Thus, the present findings should not be viewed as potential risk posed by low dietary exposure in the normal population, yet rather considered in the context of acute severe PA poisonings. This study substantially contributes to the elucidation of the mode of action of acute intoxication with senecionine as a representative of hepatotoxic PAs.

Acknowledgements This work was supported by the German Research Foundation (Grant Number LA1177/12-1), by the German Federal Institute for Risk Assessment (Grant Numbers 1322-591 and 1322-624) and the BMBF funded project LiSyM. ERL mice were generated under Cancer Research UK Programme Grant C4639/A10822 awarded to Professor C.R. Wolf. Additionally, we thank Ms. Brigitte Begher-Tibbe (Leibniz Research Center for Working Environment and Human Factors, Technical University Dortmund, Germany) for Immunostaining and for 3 D reconstructions. Special thanks to Ms. Gisela H. Degen for scientific discussion and proof reading of the manuscript.

Funding This work was supported by the German Research Foundation (Grant Number LA1177/12-1), by the German Federal Institute for Risk Assessment (Grant Numbers 1322-591 and 1322-624) and the BMBF Funded project LiSyM. ERL mice were generated under Cancer Research UK Programme Grant C4639/A10822 awarded to Professor C.R. Wolf.

Compliance with ethical standards

Conflict of interest The authors declare that they have no conflict of interest.

References

Baker DC, Pfister JA, Molyneux RJ, Kechele P (1991) Cynoglossum officinale toxicity in calves. J Comp Pathol 104(4):403–410

Bodi D, Ronczka S, Gottschalk C et al (2014) Determination of pyrrolizidine alkaloids in tea, herbal drugs and honey. Food Addit Contam Part A Chem Anal Control Expo Risk Assess 31(11):1886–1895. https://doi.org/10.1080/19440049.2014.964337

Chen Z, Huo JR (2010) Hepatic veno-occlusive disease associated with toxicity of pyrrolizidine alkaloids in herbal preparations. Neth J Med 68(6):252–260

Constien R, Forde A, Liliensiek B et al (2001) Characterization of a novel EGFP reporter mouse to monitor Cre recombination as demonstrated by a Tie2 Cre mouse line. Genesis 30(1):36–44

Copple BL, Rondelli CM, Maddox JF, Hoglen NC, Ganey PE, Roth RA (2004) Modes of cell death in rat liver after monocrotaline exposure. Toxicol Sci 77(1):172–182. https://doi.org/10.1093/toxsci/kfh011

Datta DV, Khuroo MS, Mattocks AR, Aikat BK, Chhuttani PN (1978) Herbal medicines and veno-occlusive disease in India. Postgrad Med J 54(634):511–515. https://doi.org/10.1136/pgmj.54.634.511

DeLeve LD, Shulman HM, McDonald GB (2002) Toxic injury to hepatic sinusoids: sinusoidal obstruction syndrome (veno-occlusive disease). Semin Liver Dis 22(1):27–42. https://doi.org/10.1055/s-2002-23204

DeLeve LD, Ito Y, Bethea NW, McCuskey MK, Wang X, McCuskey RS (2003a) Embolization by sinusoidal lining cells obstructs the microcirculation in rat sinusoidal obstruction syndrome. Am J Physiol Gastrointest Liver Physiol 284(6):G1045–G1052. https://doi.org/10.1152/ajpgi.00526.2002

Deleve LD, Wang X, Tsai J, Kanel G, Strasberg S, Tokes ZA (2003b) Sinusoidal obstruction syndrome (veno-occlusive disease) in the rat is prevented by matrix metalloproteinase inhibition. Gastroenterology 125(3):882–890

Denk W, Strickler J, Webb W (1990) Two-photon laser scanning fluorescence microscopy. Science 248(4951):73–76. https://doi.org/10.1126/science.2321027

Dusemund B, Nowak N, Sommerfeld C, Lindtner O, Schafer B, Lampen A (2018) Risk assessment of pyrrolizidine alkaloids in food of plant and animal origin. Food Chem Toxicol 115:63–72. https://doi.org/10.1016/j.fct.2018.03.005

Ebmeyer J, Behrend J, Lorenz M et al (2019a) Pyrrolizidine alkaloid-induced alterations of prostanoid synthesis in human endothelial cells. Chem Biol Interact 298:104–111. https://doi.org/10.1016/j.cbi.2018.11.007

Ebmeyer J, Braeuning A, Glatt H, These A, Hessel-Pras S, Lampen A (2019b) Human CYP3A4-mediated toxification of the pyrrolizidine alkaloid lasiocarpine. Food Chem Toxicol 130:79–88. https://doi.org/10.1016/j.fct.2019.05.019

Ebmeyer J, Franz L, Lim R et al (2019c) Sensitization of human liver cells toward fas-mediated apoptosis by the metabolically activated pyrrolizidine alkaloid lasiocarpine. Mol Nutr Food Res. https://doi.org/10.1002/mnfr.201801206

EFSA (2016) Dietary exposure assessment to pyrrolizidine alkaloids in the European population. EFSA J 14(8):50

Fox DW, Hart MC, Bergeson PS, Jarrett PB, Stillman AE, Huxtable RJ (1978) Pyrrolizidine (Senecio) intoxication mimicking Reye syndrome. J Pediatr 93(6):980–982. https://doi.org/10.1016/S0022-3476(78)81227-X

Fu PP, Xia Q, Lin G, Chou MW (2004) Pyrrolizidine alkaloids—genotoxicity, metabolism enzymes, metabolic activation, and mechanisms. Drug Metab Rev 36(1):1–55. https://doi.org/10.1081/DMR-120028426

Gao H, Li N, Wang JY, Zhang SC, Lin G (2012) Definitive diagnosis of hepatic sinusoidal obstruction syndrome induced by pyrrolizidine alkaloids. J Dig Dis 13(1):33–39. https://doi.org/10.1111/j.1751-2980.2011.00552.x

Gordon GJ, Coleman WB, Grisham JW (2000) Bax-mediated apoptosis in the livers of rats after partial hepatectomy in the retrorsine model of hepatocellular injury. Hepatology 32(2):312–320. https://doi.org/10.1053/jhep.2000.9144

Helmchen F, Denk W (2005) Deep tissue two-photon microscopy. Nat Methods 2(12):932–940. https://doi.org/10.1038/nmeth818

Helmy A (2006) Review article: updates in the pathogenesis and therapy of hepatic sinusoidal obstruction syndrome. Aliment Pharmacol Ther 23(1):11–25. https://doi.org/10.1111/j.1365-2036.2006.02742.x

Henderson CJ, McLaughlin LA, Osuna-Cabello M et al (2015) Application of a novel regulatable Cre recombinase system to define the role of liver and gut metabolism in drug oral bioavailability. Biochem J 465(3):479–488. https://doi.org/10.1042/bj20140582

Kakar F, Akbarian Z, Leslie T et al (2010) An outbreak of hepatic veno-occlusive disease in Western Afghanistan associated with exposure to wheat flour contaminated with pyrrolizidine alkaloids. J Toxicol 2010:313280. https://doi.org/10.1155/2010/313280

Koni PA, Joshi SK, Temann UA, Olson D, Burkly L, Flavell RA (2001) Conditional vascular cell adhesion molecule 1 deletion in mice: impaired lymphocyte migration to bone marrow. J Exp Med 193(6):741–754

Luckert C, Hessel S, Lenze D, Lampen A (2015) Disturbance of gene expression in primary human hepatocytes by hepatotoxic pyrrolizidine alkaloids: a whole genome transcriptome analysis. Toxicol In Vitro 29(7):1669–1682. https://doi.org/10.1016/j.tiv.2015.06.021

Mendel VE, Witt MR, Gitchell BS et al (1988) Pyrrolizidine alkaloid-induced liver disease in horses: an early diagnosis. Am J Vet Res 49(4):572–578

Merz KH, Schrenk D (2016) Interim relative potency factors for the toxicological risk assessment of pyrrolizidine alkaloids in food and herbal medicines. Toxicol Lett 263:44–57. https://doi.org/10.1016/j.toxlet.2016.05.002

Mohabbat O, Younos MS, Merzad AA, Srivastava RN, Sediq GG, Aram GN (1976) An outbreak of hepatic veno-occlusive disease in north-western Afghanistan. Lancet (London, England) 2(7980):269–271

Mulder PPJ, Sánchez PL, These A, Preiss-Weigert A, Castellari M (2015) Occurrence of pyrrolizidine alkaloids in food. EFSA Support Publ. 12(8):859E. https://doi.org/10.2903/sp.efsa.2015.en-859

Muzumdar MD, Tasic B, Miyamichi K, Li L, Luo L (2007) A global double-fluorescent Cre reporter mouse. Genesis 45(9):593–605. https://doi.org/10.1002/dvg.20335

Park BK, Kitteringham NR, Maggs JL, Pirmohamed M, Williams DP (2005) The role of metabolic activation in drug-induced hepatotoxicity. Annu Rev Pharmacol Toxicol 45:177–202. https://doi.org/10.1146/annurev.pharmtox.45.120403.100058

Pei QL, Kobayashi Y, Tanaka Y et al (2002) Increased expression of multidrug resistance-associated protein 1 (mrp1) in hepatocyte basolateral membrane and renal tubular epithelia after bile duct ligation in rats. Hepatol Res 22(1):58–64

Reif R, Karlsson J, Gunther G et al (2015) Bile canalicular dynamics in hepatocyte sandwich cultures. Arch Toxicol 89(10):1861–1870. https://doi.org/10.1007/s00204-015-1575-9

Reif R, Ghallab A, Beattie L et al (2017) In vivo imaging of systemic transport and elimination of xenobiotics and endogenous molecules in mice. Arch Toxicol 91(3):1335–1352. https://doi.org/10.1007/s00204-016-1906-5

Ruan J, Yang M, Fu P, Ye Y, Lin G (2014) Metabolic activation of pyrrolizidine alkaloids: insights into the structural and enzymatic basis. Chem Res Toxicol 27(6):1030–1039. https://doi.org/10.1021/tx500071q

Steenkamp V, Stewart MJ, van der Merwe S, Zuckerman M, Crowther NJ (2001) The effect of Senecio latifolius a plant used as a South African traditional medicine, on a human hepatoma cell line. J Ethnopharmacol 78(1):51–58. https://doi.org/10.1016/S0378-8741(01)00321-X

Stegelmeier BL, Gardner DR, James LF, Molyneux RJ (1996) Pyrrole detection and the pathologic progression of Cynoglossum

officinale (houndstongue) poisoning in horses. J Vet Diagn Invest 8(1):81–90. https://doi.org/10.1177/104063879600800113
Stegelmeier BL, Edgar JA, Colegate SM et al (1999) Pyrrolizidine alkaloid plants, metabolism and toxicity. J NatToxins 8(1):95–116
Stillman AS, Huxtable R, Consroe P, Kohnen P, Smith S (1977) Hepatic veno-occlusive disease due to pyrrolizidine (Senecio) poisoning in Arizona. Gastroenterology 73(2):349–352
Tandon HD, Tandon BN, Mattocks AR (1978) An epidemic of veno-occlusive disease of the liver in Afghanistan Pathologic features. Am J Gastroenterol 70(6):607–613
Waizenegger J, Braeuning A, Templin M, Lampen A, Hessel-Pras S (2018) Structure-dependent induction of apoptosis by hepatotoxic pyrrolizidine alkaloids in the human hepatoma cell line HepaRG: single versus repeated exposure. Food Chem Toxicol 114:215–226. https://doi.org/10.1016/j.fct.2018.02.036
Wang X, Kanel GC, DeLeve LD (2000) Support of sinusoidal endothelial cell glutathione prevents hepatic veno-occlusive disease in the rat. Hepatology 31(2):428–434. https://doi.org/10.1002/hep.510310224
WHO (1988) WHO IPCS International Programme on Chemical Safety: Pyrrolizidine alkaloids Environmental Health Criteria, vol 80. World Health Organization, Geneva
Xiong A, Yang F, Fang L et al (2014) Metabolomic and genomic evidence for compromised bile acid homeostasis by senecionine, a hepatotoxic pyrrolizidine alkaloid. Chem Res Toxicol 27(5):775–786. https://doi.org/10.1021/tx400451q
Yang M, Ruan J, Fu PP, Lin G (2016) Cytotoxicity of pyrrolizidine alkaloid in human hepatic parenchymal and sinusoidal endothelial cells: firm evidence for the reactive metabolites mediated pyrrolizidine alkaloid-induced hepatotoxicity. Chem Biol Interact 243:119–126. https://doi.org/10.1016/j.cbi.2015.09.011